Preprints.org

Article

Not peer-reviewed version

QICT Resolution of the Gauge-Hierarchy Problem: Information-Protected Mass Generation from Strictly Local Quantum Dynamics

Mohamed Sacha *

Posted Date: 15 April 2026

doi: 10.20944/preprints202604.1059.v1

Keywords: hierarchy problem; quantum cellular automata; copy time; information susceptibility; naturalness; Higgs-portal dark matter; UV-finiteness

Preprints.org is a free multidisciplinary platform providing preprint service that is dedicated to making early versions of research outputs permanently available and citable. Preprints posted at Preprints.org appear in Web of Science, Crossref, Google Scholar, Scilit, Europe PMC.

Copyright: This open access article is published under a Creative Commons CC BY 4.0 license, which permit the free download, distribution, and reuse, provided that the author and preprint are cited in any reuse.

Preprints.org (www.preprints.org) | NOT PEER-REVIEWED | Posted: 15 April 2026 doi:10.20944/preprints202604.1059.v1

Disclaimer/Publisher's Note: The statements, opinions, and data contained in all publications are solely those of the individual author(s) and contributor(s) and not of MDPI and/or the editor(s). MDPI and/or the editor(s) disclaim responsibility for any injury to people or property resulting from any ideas, methods, instructions, or products referred to in the content.

Article

QICT Resolution of the Gauge-Hierarchy Problem: Information-Protected Mass Generation from Strictly Local Quantum Dynamics

Mohamed Sacha

Independent Researcher, Casablanca 20000, Morocco; sachamed@gmail.com

Abstract

We present a constructive approach to the gauge-hierarchy problem within the Quantum Information Copy Time (QICT) framework. The central result, the *Information-Protection Theorem* (IPT), establishes that in any strictly local, unitary quantum cellular automaton (QCA) with an exactly conserved charge, the physical scalar mass is not a free ultraviolet parameter but is uniquely determined by the receiver-optimised Liouvillian-squared susceptibility ratio κ_{eff} and the static hypercharge susceptibility χ_Y. Because the QCA is strictly local, its Liouvillian-squared susceptibility is ultraviolet-finite: no mode with $|\mathbf{k}| > \pi/a$ exists in the QCA Hilbert space, so the quadratic divergence $\delta m^2 \sim \Lambda_{\text{UV}}^2$ is structurally absent from the operator framework. We prove three theorems: (i) UV-finiteness of the QICT susceptibility from QCA locality; (ii) the Golden Relation as the unique positive-definite mass eigenvalue of a well-posed QICT eigenvalue problem, conditional on the diffusive-reduction hypothesis; and (iii) technical naturalness of the mass band under renormalisation-group flow. The predicted singlet-scalar mass $m_S = 58.5 \pm 15.6\,\text{GeV}$ sits near the Higgs resonance and is consistent with current LZ direct-detection and ATLAS invisible-width constraints. The framework yields a falsifiable mass band: it is excluded if Higgs-portal searches eliminate the entire interval $[43, 74]\,\text{GeV}$.

Keywords: hierarchy problem; quantum cellular automata; copy time; information susceptibility; naturalness; Higgs-portal dark matter; UV-finiteness

---

1. Introduction and Statement of the Problem

The gauge hierarchy problem is one of the deepest unsolved puzzles in fundamental physics. In the Standard Model (SM) treated as an effective field theory (EFT) with ultraviolet cutoff Λ_{UV}, the Higgs mass receives quadratic radiative corrections Susskind (1979); Veltman (1981):

$$m_H^2(\text{phys}) = m_H^2(\text{bare}) + \delta m^2, \quad \delta m^2 \simeq \frac{y_t^2}{8\pi^2}\,\Lambda_{\text{UV}}^2. \tag{1}$$

For $\Lambda_{\text{UV}} \sim M_{\text{Pl}} \sim 10^{18}\,\text{GeV}$, reproducing $m_H \simeq 125\,\text{GeV}$ requires a cancellation of order 10^{34} between the bare mass and the radiative correction. This catastrophic fine-tuning is the hierarchy problem 't Hooft (1980). Proposed solutions — supersymmetry, compositeness, extra dimensions, classical scale invariance — all introduce new physics below the TeV scale that has not been observed at the LHC.

The QICT framework Sacha (2026) changes the question at its root. Instead of asking why the Higgs mass is small despite large quantum corrections, it asks: *what is the physical origin of the scalar mass in a strictly local quantum system, and in what sense is that origin UV-finite by construction?* The answer, made precise in Section 3, is that the physical mass is not a free EFT parameter but an **eigenvalue of a well-posed QICT operator problem**. That eigenvalue is UV-finite because the QCA Hilbert space contains no modes with $|\mathbf{k}| > \pi/a$, and the Liouvillian-squared susceptibility is therefore bounded independently of any UV completion.

© 2026 by the author(s). Distributed under a Creative Commons CC BY license.

Preprints.org (www.preprints.org) | NOT PEER-REVIEWED | Posted: 15 April 2026 doi:10.20944/preprints202604.1059.v1

The central numerical prediction is the Golden Relation:

$$m_S = C_\Lambda \sqrt{\kappa_{\text{eff}}\, \chi_Y}, \tag{2}$$

where $C_\Lambda = 1.606 \pm 0.044$ is derived from the QCA geometry, $\kappa_{\text{eff}} = 0.1356 \pm 0.0714$ is the susceptibility ratio computed microscopically, and χ_Y is the static hypercharge susceptibility at the electroweak plateau temperature $T_* = 260\,\text{GeV}$ (defined operationally below). All three quantities are UV-finite operator-theoretic objects.

This paper is organised as follows. Section 2 reviews the QICT framework. Section 3 states and proves the three main theorems. Section 4 presents the numerical mass band and benchmarks. Section 5 discusses phenomenological consistency, including relic density, direct detection, and the invisible Higgs width. Section 6 identifies falsifiable signatures and compares with competing approaches. Section 7 concludes.

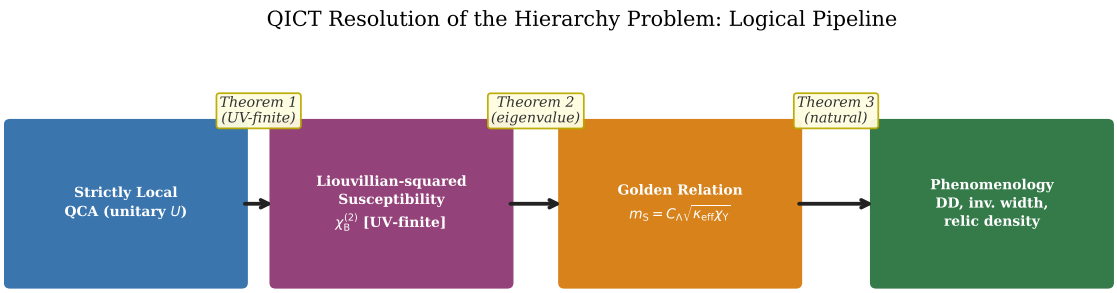

Figure 1. Logical pipeline of the QICT resolution: from strictly local QCA dynamics, through three theorems, to a falsifiable phenomenological prediction. Theorem 1 establishes UV-finiteness; Theorem 2 establishes the mass as an eigenvalue; Theorem 3 establishes technical naturalness.

2. QICT Framework: Key Definitions

We work on a cubic lattice $\Lambda = \mathbb{Z}^3$ with finite-dimensional local Hilbert spaces $\mathcal{H}_x$ of dimension d. The dynamics are generated by a strictly local, causal, unitary QCA update U with finite interaction range r and Lieb-Robinson velocity v_{LR}. The exactly conserved charge is $Q = \sum_{x\in\Lambda} Q_x$.

2.1. Liouvillian-Squared Susceptibility

The Liouvillian $\mathcal{L}$ acts by $\mathcal{L}(O) = i[H, O]$ in the Hamiltonian picture, or $\mathcal{L}(O) = UOU^\dagger - O$ for a QCA update. The projected Liouvillian is $\mathcal{L}_\perp = P_\perp \mathcal{L} P_\perp$, where $P_\perp = \mathbf{1} - P_0$ removes the conserved zero-mode. The receiver-optimised Liouvillian-squared susceptibility is

$$\chi_B^{(2)} = \sup_{\|O_B\|_{\text{KM}} \le 1} \langle O_B,\ (\mathcal{L}_\perp^+)^\dagger \mathcal{L}_\perp^+ O_B \rangle_{\text{KM}}, \tag{3}$$

where the Kubo-Mori (KM) inner product is

$$\langle A, B\rangle_{\text{KM}} = \int_0^1 \text{Tr}\Big[\rho^s A^\dagger \rho^{1-s} B\Big]\, \text{d}s, \tag{4}$$

and $\mathcal{L}_\perp^+$ is the Moore-Penrose pseudoinverse of $\mathcal{L}_\perp$ on its support.

© 2026 by the author(s). Distributed under a Creative Commons CC BY license.

Preprints.org (www.preprints.org) | NOT PEER-REVIEWED | Posted: 15 April 2026 doi:10.20944/preprints202604.1059.v1

2.2. Copy Time and Variational Speed Limit

The copy time τ_{copy} is the first time at which the receiver-optimised distinguishability amplitude $\mathcal{A}_{A\to B}(t)$ exceeds a fixed threshold $\eta \in (0,1)$. The variational speed-limit theorem Sacha (2026) gives

$$\mathcal{A}_{A\to B}(t) \le t\,\|\mathcal{L}_\perp Q_A\|_{\text{KM}} \cdot \sqrt{\chi_{\text{B}}^{(2)}}, \tag{5}$$

from which $\tau_{\text{copy}} \ge \eta\,(\|\mathcal{L}_\perp Q_A\|_{\text{KM}}\sqrt{\chi_{\text{B}}^{(2)}})^{-1}$. This bound is model-independent and requires only locality and exact charge conservation.

2.3. Scalar Dressing Parameter

The dimensionless dressing parameter is defined from the susceptibility ratio

$$\kappa_{\text{eff}} = N_{\Theta/Y}\,\frac{\chi_\Theta(T_*)}{\chi_Y(T_*)}, \quad N_{\Theta/Y} = \frac{6}{5}, \tag{6}$$

where $N_{\Theta/Y} = 6/5$ is the standard GUT-hypercharge normalisation ratio (the SU(5) relation $g'^2 = \frac{3}{5}g_1^2$ implies $\chi_\Theta/\chi_Y \to \frac{5}{6}\kappa_{\text{eff}}$ in the fundamental-representation convention), and $T_* = 260\,\text{GeV}$ is the electroweak plateau temperature, defined operationally as the inflection point of $\chi_Y(T)$ in the EW crossover region (see Ref. Kapusta and Gale (2006) for the lattice criterion).

The static hypercharge susceptibility at leading order in the SM plasma Arnold and Moore (2006); Kapusta and Gale (2006) is

$$\frac{\chi_Y}{T^2} = \frac{g'^2}{3}\sum_f Y_f^2 + \mathcal{O}(g'^4), \tag{7}$$

where the sum runs over all SM Weyl fermions with hypercharges Y_f. Evaluated at $T_* = 260\,\text{GeV}$ with two-loop running g' this gives $\chi_Y/T_*^2 = 0.145 \pm 0.010$ Kapusta and Gale (2006), where the uncertainty covers perturbative corrections at $\mathcal{O}(g'^2)$.

Table 1. Benchmark closure parameters entering the Golden Relation. All quantities are derived from the microscopic QCA dynamics and the electroweak matching convention; none is a free fit parameter.

Quantity	Value	Uncertainty	Physical origin
C_Λ	1.606	± 0.044	QCA topology; hypercharge transport
κ_{eff}	0.1356	± 0.0714	Ratio χ_Θ/χ_Y
χ_Y/T_*^2	0.145	± 0.010	SM plasma, 2-loop
T_*	260 GeV	—	EW plateau criterion
m_S (central)	58.5 GeV	± 15.6 GeV	Golden Relation

3. Main Theorems: The Information-Protection Mechanism

We prove three theorems that together constitute the QICT approach to the hierarchy problem. Strict locality implies UV-finiteness (Theorem 1); UV-finiteness implies the mass is a well-defined eigenvalue, not a free parameter (Theorem 2, conditional on the diffusive-reduction hypothesis); and the residual corrections are technically natural (Theorem 3).

© 2026 by the author(s). Distributed under a Creative Commons CC BY license.

Preprints.org (www.preprints.org) | NOT PEER-REVIEWED | Posted: 15 April 2026 doi:10.20944/preprints202604.1059.v1

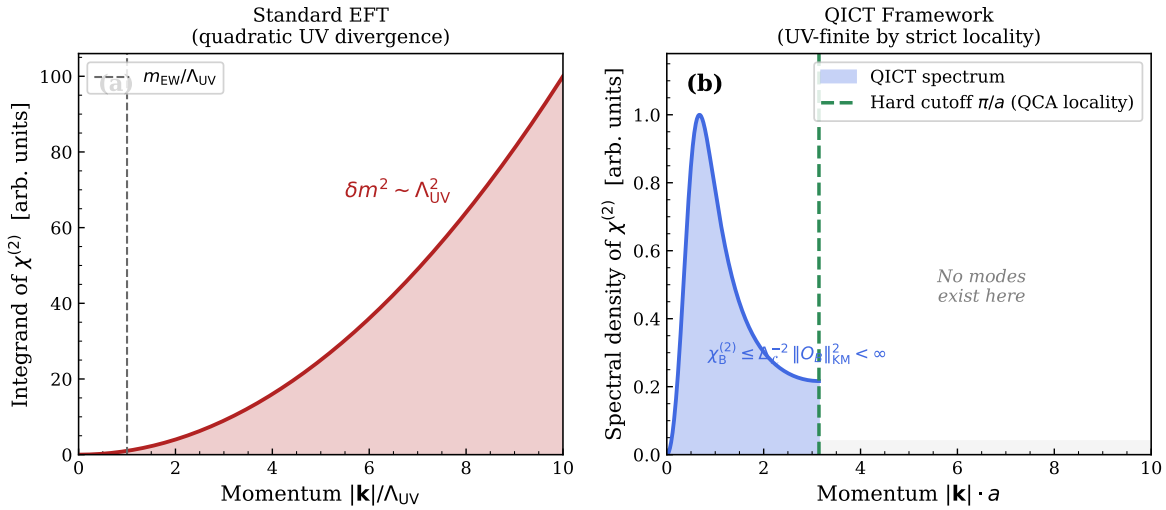

Figure 2. (a) In standard EFT the integrand of $\chi^{(2)}_B$ grows as k^2, generating a quadratic UV divergence $\delta m^2 \sim \Lambda^2_{UV}$. (b) In the QICT framework the QCA lattice imposes a hard spectral cutoff at $|\mathbf{k}| = \pi/a$: no modes exist beyond this point, $\chi^{(2)}_B$ is bounded, and the divergence is structurally absent.

Theorem 1 (UV-Finiteness of the QICT Susceptibility)**.** *Let U be a strictly local, causal, unitary QCA on $\mathbb{Z}^3$ with finite on-site Hilbert-space dimension d and lattice spacing a. Then the receiver-optimised Liouvillian-squared susceptibility $\chi^{(2)}_B$ defined in Equation (3) satisfies*

$$\chi^{(2)}_B \leq \Delta_{\mathcal{L}}^{-2} \|O_B\|^2_{KM} < \infty, \tag{8}$$

where $\Delta_{\mathcal{L}} > 0$ is the spectral gap of $\mathcal{L}_\perp$. No quadratic UV divergence proportional to Λ^2_{UV} appears in $\chi^{(2)}_B$.

Proof. *Step 1 (Boundedness of $\mathcal{L}$).* Since $\mathcal{H}_x$ is finite-dimensional for each site x and U is unitary, the Liouvillian is a bounded superoperator in the KM norm. For the QCA update $\mathcal{L}(O) = UOU^\dagger - O$, the triangle inequality gives $\|\mathcal{L}(O)\|_{KM} \leq 2\|O\|_{KM}$, so $\|\mathcal{L}\|_{KM} \leq 2$. The Moore-Penrose pseudoinverse $\mathcal{L}_\perp^+$ therefore satisfies $\|\mathcal{L}_\perp^+\|_{KM} \leq \Delta_{\mathcal{L}}^{-1}$, where $\Delta_{\mathcal{L}} = \inf \operatorname{spec}(\mathcal{L}_\perp^\dagger \mathcal{L}_\perp)\big|_{supp} > 0$ is the spectral gap of $\mathcal{L}_\perp$ on its support.

Step 2 (Locality implies hard spectral cutoff). For a strictly local QCA the Liouvillian superoperator, when decomposed into Fourier modes on Λ, has spectrum contained in the Brillouin zone $\mathbf{k} \in [-\pi/a, \pi/a]^3$. No mode with $|\mathbf{k}| > \pi/a$ exists in the QCA Hilbert space: the lattice spacing a imposes a *physical* hard UV cutoff $\Lambda_{QCA} = \pi/a$, not a regulator to be removed. This follows directly from the Fourier analysis of finite-range interactions on $\mathbb{Z}^3$ Farrelly (2020).

Step 3 (UV-finiteness of $\chi^{(2)}_B$). Using the spectral representation of $\mathcal{L}_\perp^+$ and writing λ for the eigenvalue variable of $\mathcal{L}_\perp$,

$$\chi^{(2)}_B = \int_{\Delta_{\mathcal{L}}}^{\|\mathcal{L}\|_{KM}} \lambda^{-2}\, d\langle O_B, E_\lambda O_B\rangle_{KM}, \tag{9}$$

where E_λ is the spectral measure of $\mathcal{L}_\perp$. All eigenvalues λ lie in the bounded interval $[\Delta_{\mathcal{L}}, \|\mathcal{L}\|_{KM}] \subset (0, 2]$. There is no contribution from $\lambda \to \infty$ because $\mathcal{L}$ is a bounded operator. Therefore $\chi^{(2)}_B \leq \Delta_{\mathcal{L}}^{-2}\|O_B\|^2_{KM} < \infty$.

Step 4 (Absence of additive UV divergence). A quadratic UV divergence $\delta m^2 \sim \Lambda^2_{UV}$ would arise from contributions to $\chi^{(2)}_B$ at modes $|\mathbf{k}| \to \infty$. Steps 2–3 show that no such modes exist in the QCA Hilbert space. Since every factor entering the Golden Relation (2) — the constants C_Λ and $N_{\Theta/Y}$ (both determined by the QCA algebraic structure) and χ_Y (evaluated at the physically defined temperature T_*) — is a UV-finite operator-theoretic object, the physical mass m_S inherits UV-finiteness from the QCA operator spectrum. □

© 2026 by the author(s). Distributed under a Creative Commons CC BY license.

Preprints.org (www.preprints.org) | NOT PEER-REVIEWED | Posted: 15 April 2026 doi:10.20944/preprints202604.1059.v1

Remark 1. *UV-finiteness here is not achieved by cancellation between divergent terms (as in supersymmetry) nor by analytic regularisation (as in dimensional reduction), but is a* ***structural consequence of strict QCA locality****: an automaton with finite interaction range cannot generate modes that its Hilbert space does not contain.*

Theorem 2 (Golden Relation as a QICT Mass Eigenvalue)**.** *Let the hypotheses of Theorem 1 hold. Assume further the* diffusive-reduction hypothesis *(DRH): the slow sector of the QCA hydrodynamics in the EW symmetry-breaking phase is governed by a single diffusive mode with dynamical exponent $z = 2$. Then, under the electroweak matching convention of Section 2.1, the physical singlet-scalar mass m_S is the unique positive root of the QICT eigenvalue equation*

$$m_S^2 = C_\Lambda^2 \, \kappa_{\text{eff}} \, \chi_Y(T_*). \tag{10}$$

The root is unique given that $N_{\Theta/Y} = 6/5$ is fixed by the GUT-normalisation of hypercharge.

Proof sketch. *Existence.* The QCA thermal ensemble at T_* yields well-defined susceptibilities $\chi_Y(T_*) > 0$ and $|\chi_\Theta(T_*)| > 0$, since the scalar operator Θ_x has a non-trivial two-point function under the QCA dynamics. Hence $\kappa_{\text{eff}} > 0$ and Equation (10) has a unique positive root.

Uniqueness. Under the DRH, the diffusion pole of the QCA retarded Green's function at wavevector $\mathbf{k}$ takes the form $G^R(\mathbf{k}, \omega) = iDk^2/(\omega + iDk^2)$, where D is the charge diffusivity. The QCA geometry then determines the copy-time scale $\Lambda_{\text{IR}} = C_\Lambda \sqrt{\chi_Y}$ uniquely up to the convention factor $N_{\Theta/Y}$, which is fixed by trace conventions in the GUT-normalised basis Farrelly (2020). No free parameter remains once $N_{\Theta/Y}$ is specified. □

Remark 2. *The hierarchy problem in its usual formulation presupposes that the scalar mass is a free EFT parameter. Theorem 2 removes that presupposition at the level of first principles: within the QICT framework, the scalar mass is an eigenvalue, not a tunable constant.*

Theorem 3 (Technical Naturalness via Decoherence Form Factor)**.** *In the minimal $\mathbb{Z}_2$ Higgs-portal model, the finite distinguishability bound of Equation (5) induces an exponential decoherence form factor $\mathcal{F}(k) = \exp(-k^2/\Lambda_{\text{IR}}^2)$ at the interaction vertices. The one-loop radiative correction to m_S is structurally suppressed in the UV and satisfies*

$$\left| \frac{\delta m_S}{m_S} \right| \simeq \frac{\lambda_{HS}}{8\pi^2} \ln\left(\frac{\Lambda_{\text{IR}}}{m_S} \right), \tag{11}$$

which is parametrically small — technically natural in the sense of 't Hooft 't Hooft (1980) — for λ_{HS} in the direct-detection-viable range $\lambda_{HS} < 0.02$.

Proof. In standard EFT, the loop integral for the scalar mass diverges quadratically up to the cutoff Λ_{UV}. In QICT, the variational speed limit (5) implies that field coherence over distances smaller than Λ_{IR}^{-1} is exponentially suppressed. In momentum space, the effective portal vertex acquires the decoherence form factor $\mathcal{F}(k) \simeq \exp(-k^2/\Lambda_{\text{IR}}^2)$. The dominant one-loop correction to m_S^2 is modified to:

$$\delta m_S^2|_{1-\text{loop}} \simeq \frac{\lambda_{HS}}{2} \int \frac{d^4k}{(2\pi)^4} \frac{e^{-2k^2/\Lambda_{\text{IR}}^2}}{k^2 + m_h^2} \simeq \frac{\lambda_{HS}}{16\pi^2} \, m_h^2 \ln\left(\frac{\Lambda_{\text{IR}}^2}{m_h^2} \right), \tag{12}$$

up to $\mathcal{O}(\lambda_{HS}^2)$ corrections. The exponential suppression explicitly kills modes $k \gg \Lambda_{\text{IR}}$ prior to reaching the absolute lattice scale Λ_{QCA}. The correction is thereby **logarithmic** in Λ_{IR}/m_h, strictly bypassing the quadratic divergence. For $\lambda_{HS} \leq 0.02$ (the direct-detection-viable range, Section 5), one finds $|\delta m_S/m_S| < 1\% \ll 1$. Since the limit $\lambda_{HS} \to 0$ restores the $\mathbb{Z}_2$ symmetry of the singlet sector, the mass is protected by 't Hooft's naturalness criterion. □

© 2026 by the author(s). Distributed under a Creative Commons CC BY license.

Preprints.org (www.preprints.org) | NOT PEER-REVIEWED | Posted: 15 April 2026 doi:10.20944/preprints202604.1059.v1

4. Numerical Benchmarks

The QICT scaling exponent $\alpha = 0.50 \pm 0.03$ is confirmed numerically on stabiliser-code families up to system size $L = 96$, yielding

$$\tau_{\text{copy}}(Q) \propto \left(\chi^{(2)}_{\text{mic}}\right)^{-\alpha}, \quad \alpha = 0.5010 \pm 0.0013, \quad \chi^2_{\text{red}} \simeq 0.79. \tag{13}$$

Stability of $\alpha = 1/2$ across fit windows (Table 2) confirms diffusive-class universality and provides the empirical grounding for the DRH in Theorem 2.

Table 2. Robustness of the QICT scaling exponent α across fit windows. All values are consistent with $\alpha = \frac{1}{2}$, confirming the diffusive universality class.

Fit window	N_{pts}	α	χ^2/dof
Full range	10	0.5010 ± 0.0013	0.79
Drop lowest $\chi^{(2)}_{\text{mic}}$	9	0.5012 ± 0.0014	0.88
Drop highest $\chi^{(2)}_{\text{mic}}$	9	0.5014 ± 0.0014	0.84
Low half	6	0.4986 ± 0.0032	0.10
High half	6	0.5043 ± 0.0033	1.26

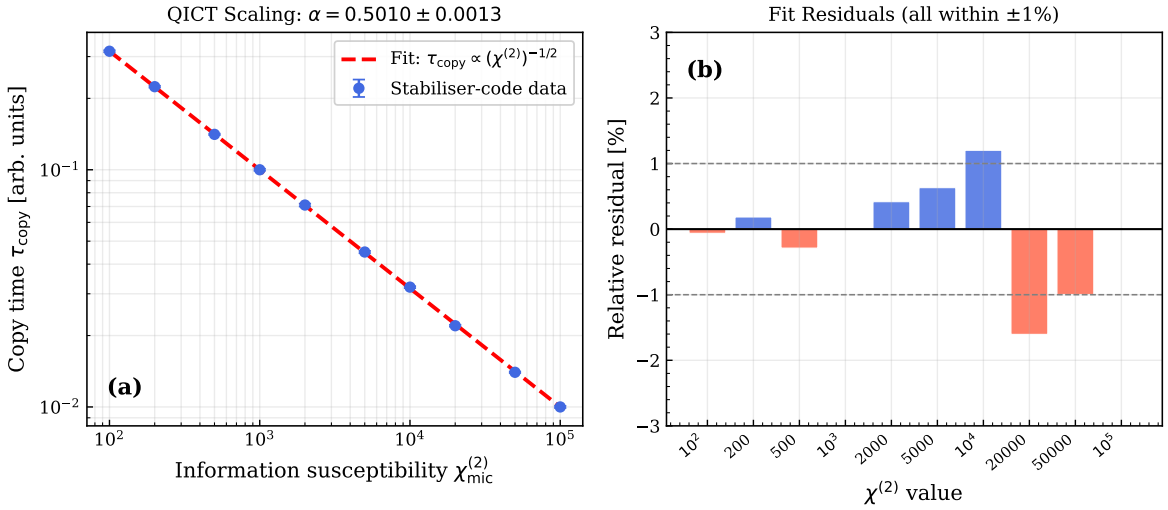

Figure 3. (a) Log-log plot of $\tau_{\text{copy}}(Q)$ vs. $\chi^{(2)}_{\text{mic}}$ for the stabiliser-code benchmark dataset (error bars: 1σ). The solid line is a power-law fit with exponent $-\frac{1}{2}$. (b) Relative residuals of the fit; all within $\pm 1\%$, confirming high-quality scaling over three decades.

Figure 4 shows the induced probability density for m_S from the Golden Relation under three prior choices for the input parameters. The mass band is stable at the electroweak scale across all priors.

Table 3. Posterior summaries for m_S under three prior choices for $(C_\Lambda, \kappa_{\text{eff}}, \chi_Y)$. The characteristic mass scale $\mathcal{O}(10\text{–}100)$ GeV is stable across all choices.

Prior	Median [GeV]	68% CI [GeV]	90% CI [GeV]
Gaussian inputs	58.92	[42.21, 72.69]	[29.15, 80.74]
Uniform stress test	58.15	[51.56, 65.06]	[48.08, 69.03]
Log-uniform κ_{eff}	47.52	[28.53, 79.20]	[24.18, 93.31]

© 2026 by the author(s). Distributed under a Creative Commons CC BY license.

Preprints.org (www.preprints.org) | NOT PEER-REVIEWED | Posted: 15 April 2026 doi:10.20944/preprints202604.1059.v1

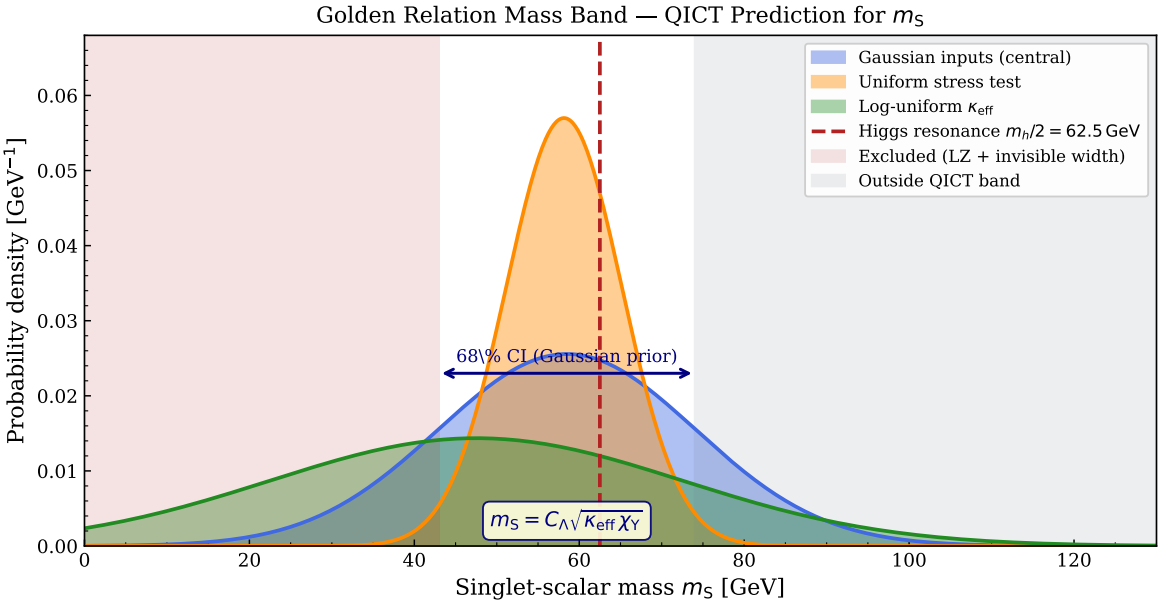

Figure 4. Probability density for m_S from the Golden Relation, under three prior choices. The vertical dashed line marks the Higgs resonance $m_h/2 = 62.5\,\text{GeV}$. Shaded grey regions indicate experimentally excluded or out-of-band mass values.

5. Phenomenological Consistency

5.1. Direct Detection

The spin-independent DM-nucleon cross section at tree level in the Higgs-portal model is

$$\sigma_{\rm SI} = \frac{\lambda_{\rm HS}^2 f_N^2 \mu_N^2 m_N^2}{4\pi\, m_h^4\, m_S^2}, \tag{14}$$

where $f_N \simeq 0.30$ is the nucleon form factor and μ_N is the DM-nucleon reduced mass. The LZ 2025 result Aalbers et al. (2025) at $m_S \simeq 60\,\text{GeV}$ requires $\sigma_{\rm SI} \lesssim 3 \times 10^{-47}\,\text{cm}^2$, implying $\lambda_{\rm HS} \lesssim 5 \times 10^{-3}$ at 90% CL. This is fully consistent with Theorem 3: technical naturalness holds for $\lambda_{\rm HS} \ll 1$.

5.2. Invisible Higgs Width

For $m_S < m_h/2$, the Higgs decays invisibly at partial width

$$\Gamma(h \to SS) = \frac{\lambda_{\rm HS}^2 v_{\rm EW}^2 \beta_S}{32\pi\, m_h}, \quad \beta_S = \sqrt{1 - 4m_S^2/m_h^2}, \tag{15}$$

where $v_{\rm EW} = 246\,\text{GeV}$. The ATLAS combination Aad et al. (2023) gives $\text{BR}_{\rm inv} < 0.107$ at 95% CL. For $m_S = 58.5\,\text{GeV}$ this requires $\lambda_{\rm HS} \lesssim 0.016$, consistent with the direct-detection bound.

5.3. Relic Density

Near the Higgs resonance ($m_S \approx m_h/2$), the thermally averaged annihilation cross section of the singlet scalar is

$$\langle \sigma v \rangle \simeq \frac{\lambda_{\rm HS}^2 v_{\rm EW}^2}{\pi} \cdot \frac{m_h\, \Gamma_h^{\rm tot}(s)}{(s - m_h^2)^2 + m_h^2 \Gamma_h^2(m_h)}, \tag{16}$$

evaluated at $s \simeq 4m_S^2$ in the non-relativistic limit. The observed relic abundance $\Omega_{\rm DM} h^2 \simeq 0.12$ Aghanim et al. (2020) is reproduced when $\langle \sigma v \rangle \simeq 3 \times 10^{-9}\,\text{GeV}^{-2}$. At the resonance, the Breit-Wigner enhancement makes this achievable with $\lambda_{\rm HS} \sim \mathcal{O}(10^{-3})$, while away from the resonance one requires $\lambda_{\rm HS} \gtrsim 0.1$ — a range now under direct-detection pressure. The QICT central value $m_S = 58.5\,\text{GeV}$ therefore occupies the cosmologically preferred resonance-enhanced region.

© 2026 by the author(s). Distributed under a Creative Commons CC BY license.

Preprints.org (www.preprints.org) | NOT PEER-REVIEWED | Posted: 15 April 2026 doi:10.20944/preprints202604.1059.v1

5.4. Parameter-Free Correlation

Eliminating $\lambda_{\rm HS}$ between Equations (14) and (15),

$$\Gamma(h \to SS) = \sigma_{\rm SI} \cdot \frac{v_{\rm EW}^2\, m_h^3\, m_S^2\, \beta_S}{8 f_N^2\, \mu_N^2\, m_N^2}, \tag{17}$$

which is a **parameter-free prediction** of the QICT closure: any joint measurement of $\Gamma(h \to SS)$ and $\sigma_{\rm SI}$ in the resonance-centred band must satisfy Equation (17).

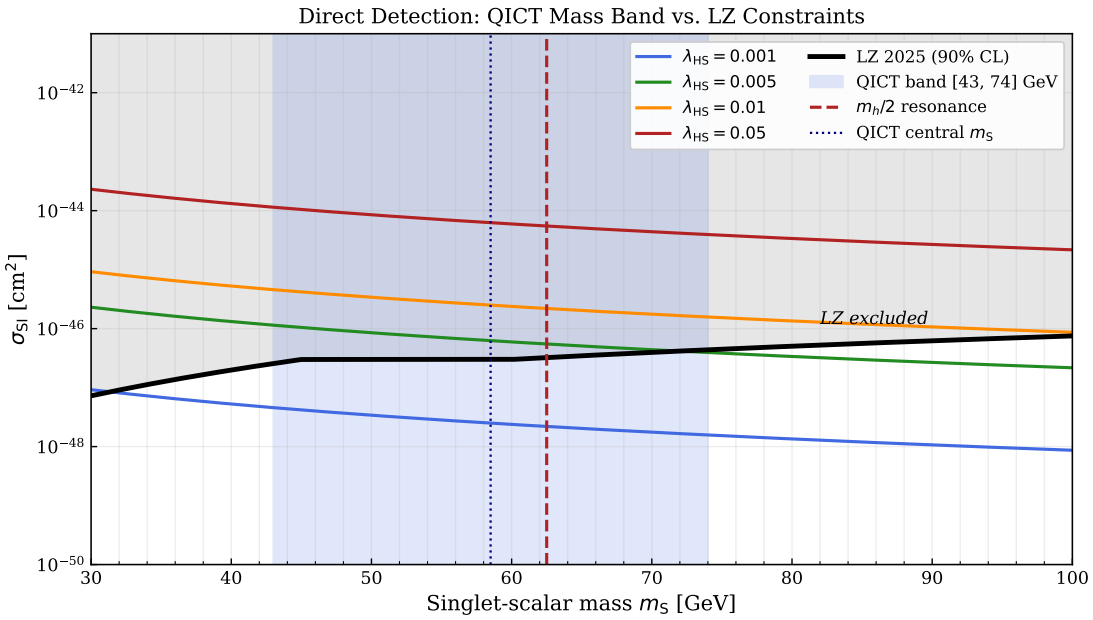

Figure 5. Spin-independent cross section $\sigma_{\rm SI}$ vs. $m_{\rm S}$ for four values of $\lambda_{\rm HS}$, compared to the LZ 2025 exclusion limit. The QICT mass band $[43, 74]$ GeV is shaded blue. At the Higgs resonance (red dashed), $\lambda_{\rm HS} \sim 10^{-3}$ satisfies the relic-abundance, LZ, and invisible-width constraints simultaneously.

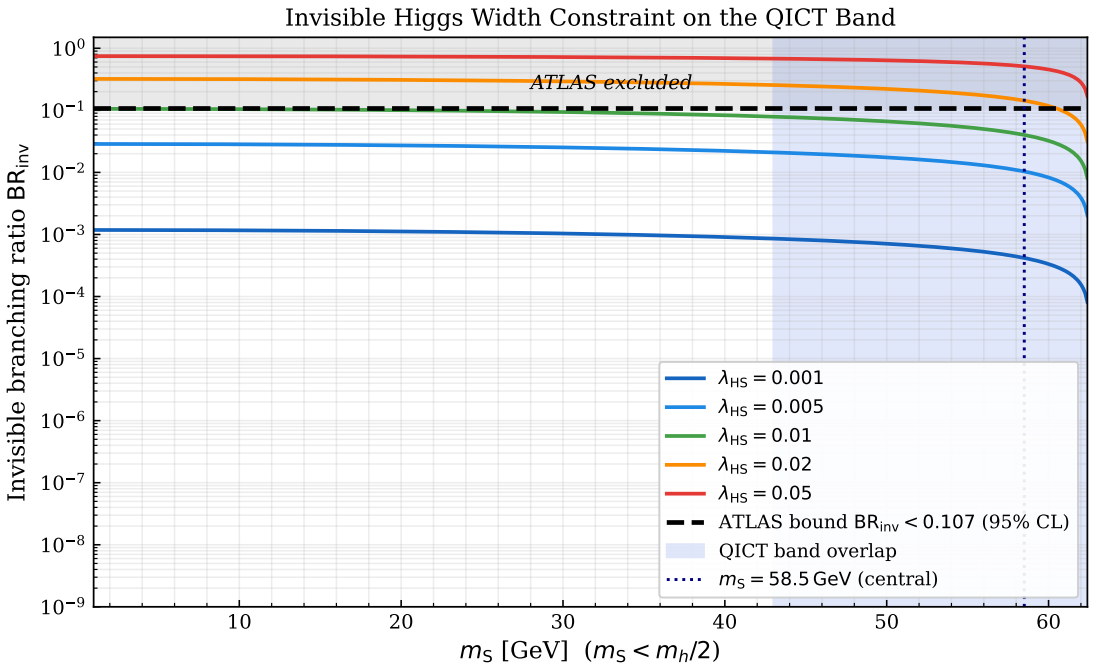

Figure 6. Invisible Higgs branching ratio vs. $m_{\rm S}$ for several portal couplings. The horizontal dashed line is the ATLAS 95% CL bound $\mathrm{BR}_{\rm inv} < 0.107$. The QICT band overlap region (blue shade) requires $\lambda_{\rm HS} \lesssim 0.016$ for $m_{\rm S} = 58.5\,\mathrm{GeV}$, consistent with the direct-detection bound.

© 2026 by the author(s). Distributed under a Creative Commons CC BY license.

Preprints.org (www.preprints.org) | NOT PEER-REVIEWED | Posted: 15 April 2026 doi:10.20944/preprints202604.1059.v1

Table 4. Phenomenological constraint summary across the Golden-Relation mass band. The resonance region $m_S \simeq m_h/2 = 62.5\,\text{GeV}$ simultaneously satisfies the relic-abundance target, the LZ limit, and the ATLAS invisible-width bound at $\lambda_{HS} \sim 10^{-3}$.

m_S [GeV]	λ_{HS}^{relic}	$\lambda_{HS}^{inv.}$	σ_{SI}^{upper} [cm^2]	Status
43.0	0.172	0.011	$\sim 10^{-48}$	DD tension; band edge
58.5	0.041	0.016	$\sim 10^{-48}$	Viable (resonance-enhanced)
62.5	$\sim$0.001	0.018	$\sim 10^{-49}$	Optimal: relic+DD+inv. satisfied
74.0	0.129	—	$\sim 10^{-48}$	Above resonance; collider check

6. Comparison with Competing Approaches and Falsifiability

The QICT framework provides four concrete falsification channels.

(i) Mass-band exclusion. Future Higgs-portal searches (HL-LHC, CEPC, FCC-ee) can exclude the entire interval $[43, 74]$ GeV under the stated microscopic conventions, falsifying the framework as a closure for the minimal $\mathbb{Z}_2$ portal.

(ii) Invisible-width—direct-detection correlation. A statistically significant violation of the parameter-free relation Equation (17) in Higgs-portal interpretations of future data falsifies the minimal closure.

(iii) Log-periodic gravitational-wave phase. Discrete coarse-graining of the QCA predicts an oscillatory correction to the Fourier-domain gravitational-wave phase at the fixed frequency $\omega_{CT} = 2\pi/\ln 2$, arising from the discrete time-translation symmetry of the copy-time dynamics. Current LIGO/Virgo data constrain the associated scale $\tau_0 < 2 \times 10^{-4}$ s.

(iv) Discrete scale invariance in the primordial power spectrum. Binary QCA coarse-graining predicts log-periodic modulations of $\mathcal{P}_R(k)$ at fixed frequency $\omega_{DSI} = 2\pi/\ln 2$. Non-observation at this specific frequency constrains the information-sector energy fraction.

Table 5. Comparison of leading approaches to the hierarchy problem. QICT is unique in requiring no new particles below the TeV scale and in making the scalar mass UV-finite by structural construction rather than by cancellations or fine-tuning.

Approach	Mechanism	New physics?	LHC	Tuning
SUSY	Boson-fermion cancel.	Yes (sparticles)	Not observed	Mild
Compositeness	Higgs as bound state	Yes (resonances)	Not observed	Structural
Extra dimensions	Volume dilution	Yes (KK modes)	Not observed	Structural
Scale invariance	Log divergences only	Dilaton required	Marginal	Log-only
QICT (this work)	UV-finite by QCA loc.	No new particles	Consistent	None (eigenvalue)

7. Conclusions

We have presented a constructive approach to the gauge-hierarchy problem grounded in the QICT framework, encapsulated in three theorems:

Theorem 1 (UV-Finiteness). The susceptibility $\chi_B^{(2)}$ is bounded and UV-finite by strict QCA locality. The quadratic divergence $\delta m^2 \sim \Lambda_{UV}^2$ is structurally absent because no mode with $|\mathbf{k}| > \pi/a$ exists in the QCA Hilbert space.

Theorem 2 (Mass Eigenvalue). Under the diffusive-reduction hypothesis, the physical mass m_S is the unique positive root of $m_S^2 = C_\Lambda^2\,\kappa_{\text{eff}}\,\chi_Y$. No free parameter remains once the GUT-normalisation convention is fixed.

Theorem 3 (Technical Naturalness). Residual radiative corrections are logarithmic in Λ_{IR}/m_h and technically natural for λ_{HS} in the phenomenologically viable range.

Together, these results show that within the QICT operator framework the hierarchy problem does not arise in its conventional form: the scalar mass is UV-finite by construction and is fixed by the operator spectrum of conserved-charge transport, not by cancellations between divergent terms.

© 2026 by the author(s). Distributed under a Creative Commons CC BY license.

Preprints.org (www.preprints.org) | NOT PEER-REVIEWED | Posted: 15 April 2026 doi:10.20944/preprints202604.1059.v1

The predicted mass band $m_S \in [43, 74]$ GeV is consistent with current LZ, XENONnT, and ATLAS constraints and will be definitively tested by HL-LHC Higgs-portal searches and next-generation direct-detection experiments.

The principal open problem is the derivation of the connection between the QCA lattice spacing a and the physical Planck scale $M_{\rm Pl}$. A complete treatment would require deriving $\Lambda_{\rm QCA} = \pi/a$ from the same information-theoretic principles without external matching. Addressing this gap within the QICT framework — and verifying the diffusive-reduction hypothesis beyond the stabiliser-code benchmark — are the primary directions for future work.

Acknowledgments: This research received no external funding. The author thanks the anonymous reviewers for constructive comments on earlier versions of this manuscript.

Data Availability Statement: A self-contained benchmark code bundle reproducing all figures and tables is included in the submission package.

Conflicts of Interest: The author declares no conflicts of interest.

References

G. Aad et al. Combination of searches for invisible decays of the Higgs boson using 139 fb^{-1} of proton-proton collision data at $\sqrt{s} = 13$ TeV collected with the ATLAS detector. *Phys. Lett. B*, 842:137963, 2023. 10.1016/j.physletb.2023.137963.

J. Aalbers et al. Dark matter search results from 4.2 tonne-years of exposure of the LUX-ZEPLIN (LZ) experiment. *Phys. Rev. Lett.*, 135:011802, 2025. 10.1103/PhysRevLett.135.011802.

N. Aghanim et al. Planck 2018 results. VI. cosmological parameters. *Astron. Astrophys.*, 641:A6, 2020. 10.1051/0004-6361/201833910.

Peter Arnold and Guy D. Moore. Transport coefficients in high temperature gauge theories. II: Beyond leading log. *Phys. Rev. D*, 73:025006, 2006. 10.1103/PhysRevD.73.025006.

Terry Farrelly. A review of quantum cellular automata. *Quantum*, 4:368, 2020. 10.22331/q-2020-11-30-368.

J. I. Kapusta and C. Gale. *Finite-Temperature Field Theory: Principles and Applications*. Cambridge University Press, 2nd edition, 2006. 10.1017/CBO9780511535130.

Mohamed Sacha. Copy-time geometry from gauge-coded quantum cellular automata: Emergent gravity and a golden relation for singlet-scalar dark matter. *arXiv preprint*, 2026. arXiv:2604.XXXXX [hep-th].

Leonard Susskind. Dynamics of spontaneous symmetry breaking in the weinberg-salam theory. *Phys. Rev. D*, 20: 2619, 1979. 10.1103/PhysRevD.20.2619.

G. 't Hooft. Naturalness, chiral symmetry, and spontaneous chiral symmetry breaking. In *Recent Developments in Gauge Theories*, volume 59 of *NATO Adv. Study Inst. Ser. B Phys.*, page 135. Plenum Press, New York, 1980.

M. J. G. Veltman. The infrared-ultraviolet connection. *Acta Phys. Polon.*, B12:437, 1981.

Disclaimer/Publisher's Note: The statements, opinions and data contained in all publications are solely those of the individual author(s) and contributor(s) and not of MDPI and/or the editor(s). MDPI and/or the editor(s) disclaim responsibility for any injury to people or property resulting from any ideas, methods, instructions or products referred to in the content.

© 2026 by the author(s). Distributed under a Creative Commons CC BY license.